Chinese Journal of
POLYMER SCIENCE

ARTICLE

https://doi.org/10.1007/s10118-018-2013-2
Chinese J. Polym. Sci. 2018, 36, 528–535

Grafting Branch Length and Density Dependent Performance of Zwitterionic Polymer Decorated Polypropylene Membrane

Jing-Jing Wu[a], Jin Zhou[a, b*], Jing-Qiu Rong[a], Yao Lu[a], Hui Dong[a], Hai-Yin Yu[a*], and Jia-Shan Gu[a]

[a] *College of Chemistry and Materials Science, Anhui Normal University, Wuhu 241000, China*
[b] *Department of Material and Chemical Engineering, Chizhou University, Chizhou 247000, China*

Abstract Branch length and density have critical effects on membrane performances; however, it is regarded to be traditionally difficult to investigate the relationship due to the uncontrolled membrane modification methods. In this study, zwitterionic polymer with controlled grafting branch chain length (degree of polymerization) and grafting density (grafting chains per membrane area) was tethered to the microporous polypropylene membrane surface based on the combination of reversible addition-fragmentation chain transfer (RAFT) polymerization technique with click reaction. The modified membranes were tested by filtrating protein dispersion to highlight the correlations of branch chain length and grafting density with the membrane permeation performances. The pure water flux, the flux recovery ratio are positively and significantly, and the irreversible fouling negatively and significantly correlated with grafting density. These results demonstrate that the larger the coverage of the membrane with poly{[2-(methacryloyloxy)ethyl]-dimethyl-(3-sulfopropyl) ammonium hydroxide} (PMEDSAH), the higher the pure water flux and the higher the flux recover ratio, and the lower the irreversible fouling, which shows that high grafting density is favorable to fouling reducing.

Keywords Grafting branch length; Grafting density; Polypropylene membrane; Protein fouling; Zwitterionic polymer

Citation: Wu, J. J.; Zhou, J.; Rong, J. Q.; Lu, Y.; Dong, H.; Yu, H. Y.; Gu, J. S. Grafting Branch Length and Density Dependent Performance of Zwitterionic Polymer Decorated Polypropylene Membrane. Chinese J. Polym. Sci. 2018, 36(4), 528–535.

INTRODUCTION

Membrane science and technology is a rapidly emerging field in chemical engineering. Membrane is the core of membrane science and technology. However, membrane fouling is the major bottleneck for its wide applications[1]. To solve this problem, membrane surface modification is widely explored to improve the membrane performance without altering the bulk specialties. Many techniques have been applied to membrane surface modification, including chemical and low temperature plasma treatment[2] and photo-induced grafting[3]. Chemically grafting chains to a polymer surface is relatively favorable due to the covalent linkage formation and thus the long-term stability[4]. However, neither the grafting density nor the grafting branch chain length, which plays a significant role in membrane performance, can be controlled in most approaches mentioned, such as UV and plasma treatment or free radical polymerization[5, 6].

The Cu^{I}-catalyzed triazo-alkynyl cycloaddition is one of the most commonly-used click reactions[7, 8], which shows high efficiency, less side reaction and high selectivity. It is vastly used in polymer synthesis currently. Polymers, with narrow polydispersity, preset molecular weight, controlled composition, and functionality, can be synthesized by the controlled free radical polymerization (CRP) techniques[9], among which the RAFT polymerization (reversible addition fragmentation transfer polymerization) can work with quite some vinyl monomers[10] under the similar mild reaction conditions to free radical polymerization; hence, RAFT is apparently the most favorable CRP. Combining RAFT polymerization with click reaction makes it possible to tailor the architectures individually and to characterize the grafting chains elaborately in great detail.

Zwitterionic polymers, which bear both a positive and a negative charge in the same unit, have been proven to be promising materials for membrane separations due to the super-hydrophilic and super-low bio-fouling characteristics[11]. It is believed that zwitterionic polymer chains resist nonspecific protein adsorption *via* a hydration layer bound through solvation of the charged terminal groups in addition to hydrogen bonding due to charge interactions[12, 13]. Consequently using zwitterionic polymers to improve the anti-fouling performance of various porous surfaces has aroused wide attention[12, 14, 15]. In our previous work, a zwitterionic polymer was introduced to the thin-film composite forward osmosis polyamide membrane by click chemistry, and excellent antifouling of Aldrich humic acid was achieved; however, effects of the branch length and grafting density on membrane characteristics have not been investigated[16]. Generally, zwitterionic polymers were

---

* Corresponding authors: E-mail zhoujin_ah@163.com (J.Z.)
E-mail yhy456@mail.ahnu.edu.cn (H.Y.Y.)

Received May 26, 2017; Accepted July 15, 2017; Published online October 30, 2017

grafted to different polymeric membrane surfaces by different methods, and the super-low fouling or biofouling characteristics were achieved. However, it is difficult to prepare and characterize the grafting chains, and as a result, the impacts of the grafting chain length and the grafting density on the membrane performances have not yet been known clearly.

In the present work, poly{[2-(methacryloyloxy)ethyl]-dimethyl-(3-sulfopropyl) ammonium hydroxide} (PMEDSAH) was grafted to the microporous polypropylene membrane (MPPM) surface *via* combining the RAFT polymerization and click technique. In the first step, the clickable membrane with triazos (MPPM-N_3) was prepared[10]; then PMEDSAH with alkynyl capped on the chain end (alkynyl-PMEDSAH), the clickable grafting chain, was prepared *via* the RAFT polymerization; finally click coupling alkynyl-PMEDSAH to MPPM-N_3 was conducted. This technique ensures the preparation of the grafting side chain individually in a controlled manner and the characterization of the grafting chain extensively, which helps to throw light on how the branch chain length (degree of polymerization) and the grafting density (grafting chains per membrane area) affect the permeation performance of the modified membranes.

EXPERIMENTAL

Materials

Microporous polypropylene membrane (MPPM, porosity about 75%, average pore size 0.20 μm, thickness 160 μm) was purchased (Membrana GmbH, Germany). Clickable microporous polypropylene membrane (triazo containing MPPM, MPPM-N_3) was fabricated as previously described[10]. Sodium ascorbate and $CuSO_4 \cdot 5H_2O$ were purchased from Sinophaim Chemical Reagent Co., Ltd and [2-(methacryloyloxy)ethyl]-dimethyl-(3-sulfopropyl) ammonium hydroxide (MEDSAH) from Sigma-Aldrich. BSA, bovine serum albumin (Sino-American Biotechnology Co., purity > 98%, isoelectric point (pI) 4.8, M_w = 66 kDa) was prepared in the phosphate buffered solution (PBS) buffer at 7.4. Alkynyl embodying chain transfer agent (alkynyl-CTA) was synthesized[17]. All of the chemicals were used as received.

Synthesis of PMEDSAH

0.0102 g (0.060 mmol) of 2,2′-azobisisobutyronitrile (AIBN), 0.0512 g (0.138 mmol) of alkynyl-CTA, 2.5 g (0.0083 mol) of MEDSAH, 14 mL of methanol, and 1 mL of DMF were mixed in a Schlenk flask. Three cycles of vacuum and nitrogen filling were conducted to get rid of O_2. The reaction was carried out at 60 °C under inert atmosphere for 24 h. The polymerization was ended by exposing the solution to air. The PMEDSAH with alkynyl capped on the end was obtained from the solution precipitated in cold ethanol. Then the polymers were re-dissolved in 15 mL 0.2 mol/L NaCl solution. The dissolution-precipitation was performed for three times, and the polymer was dried in a vacuum oven (12 h, 50 °C) into white powder.

Surface Modification of MPPM by Click Reaction

MPPM-N_3 was charged into a Schlenk flask; O_2 was removed by three-cycle vacuum and nitrogen filling. 0.50 g (0.20 mmol) of alkynyl-PMEDSAH was added to 100 mL of deionized water and 100 mL of DMF. $CuSO_4 \cdot 5H_2O$ and sodium ascorbate were used as the catalysts[10]. After reaction the membranes were washed with pure water in a shaking water bath at 30 °C for 24 h (the washed water was exchanged with fresh pure water in 30 min interval for the first 3 h), dried completely in vacuum to a constant weight and used for characterization and filtration measurements.

Grafting density of PMEDSAH (GD) is calculated with formula (1):×

$$\text{GD (chains}/100\text{nm}^2) = \frac{m_1 - m_0}{A_{\text{BET}} \times M_\eta} \times \frac{6.023 \times 10^{23}}{10^{18}} \times 100 \quad (1)$$

where m_1 (g) is the weight of MPPM-*g*-PMEDSAH, m_0 (g) the weight of the nascent MPPM, A_{BET} (m^2) Brunauer-Emmett-Teller (BET) specific surface area of the membrane (measured by Beckmann-Coulter GmbH technique, 28.5 m^2/g), M_η viscosity average molecular weight of alkynyl-PMEDSAH. All results were the means of three parallel samples.

The intrinsic viscosity of aqueous alkynyl-PMEDSAH in 0.2 mol/L NaCl aqueous solution was measured with a capillary Ubbelohde viscometer at (21.0 ± 0.2) °C (PMEDSAH is not soluble in pure water because of the charge interaction[11]), α and k are 0.4071 and 2.06×10^{-3}, respectively[11]. The degree of polymerization (DP) then can be obtained by $M_\eta/303$, where 303 is the molecular weight of MEDSAH monomer.

Characterization

Fourier transform infrared spectroscopy (FTIR, FTIR-8400S, Hitachi, Japan) was carried out (KBr pellet method) to determine the chemical structures of MEDSAH monomer and the polymer alkynyl-PMEDSAH. X-ray photoelectron spectroscopy (XPS, PHI 5000c, Perkin-Elmer Instruments, U.S.A.) was performed to identify the changes of the chemical composition of the membrane surface. The wide scan from 0 eV to 900 eV was recorded. Membrane surface morphologies were observed at 5 keV with a field emission scanning electron microscope, FESEM (Hitachi S-4800, Japan). The static sessile drop water contact angle was measured by ua contact angle system (CTS-200, Mighty Technology Pvt. Ltd., China). At least five values were taken to eradicate any discrepancies with the standard deviation at ± 5%.

Filtration Experiments

Membrane flux was measured with a dead-ended ultrafiltration device (Amicon 8050) at 20 °C, transmembrane pressure of 100 kPa and magnetic stirring speed of 200 r/min; the feed tank (1 gallon millipore) was pressurized with Ar to force the feed solution into the cell[10]. The flux recovery ratio (FRR), the relative flux reduction (RFR), reversible fouling and irreversible fouling were calculated with formulas (2)–(5):

$$\text{Flux recovery ratio } (\text{FRR, \%}) = \frac{J_1}{J_{0,\text{m}}} \times 100 \quad (2)$$

$$\text{Relative flux reduction } (\text{RFR, \%}) = \frac{J_{0,\text{m}} - J_{\text{p}}}{J_{0,\text{m}}} \times 100 \quad (3)$$

$$\text{Reversible fouling}(\%) = \frac{J_1 - J_p}{J_{0,m}} \times 100 = \text{FRR} + \text{RFR} - 100 \quad (4)$$

$$\text{Irreversible fouling}(\%) = \frac{J_{0,m} - J_1}{J_{0,m}} \times 100 = 100 - \text{FRR} \quad (5)$$

The water fluxes were normalized by Eq. (6) to elevate the differences between the original membranes:

$$\text{Normalized flux} = \frac{J_{0,m}}{J_{0,u}} \quad (6)$$

where $J_{0,u}$ and $J_{0,m}$ respectively refer to the pure water fluxes through the original membranes and the modified membranes, J_p the steady flux of BSA dispersion (1.0 g/L BSA in PBS at pH = 7.4), J_1 the deionized water fluxes after BSA-permeating and deionized water washing.

The statistics package of social science (SPSS, 19.0) was employed to analyze Pearson correlations between pendent length (PMEDSAH molecular weight) and grafting density with pure flux water, flux recovery ratio, relative flux reduction, reversible and irreversible fouling.

RESULTS AND DISCUSSION

Preparation of Alkynyl-PMEDSAH

As seen in Fig. 1, the two peaks, located at 1726 and 1480 cm^{-1}[11], are attributed to the stretching vibration of C = O and quaternary ammonium of MEDSAH and PMEDSAH. The S=O asymmetric and symmetric stretches are located at 1183 and 1046 cm^{-1}[11], and the methylene peak at 2980 cm^{-1}. A new peak appears (2092 cm^{-1}), characteristic of the alkynyl[18], arising from the chain transfer agent. The results confirm the synthesis of clickable PMEDSAH *via* RAFT polymerization.

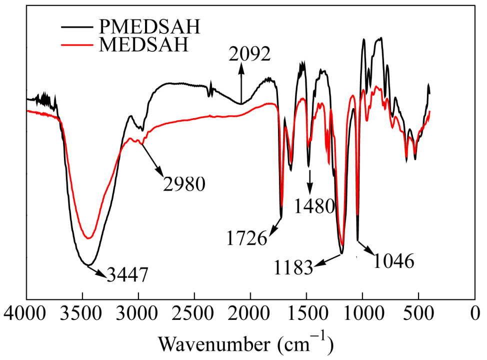

Fig. 1 FTIR spectra of MEDSAH and PMEDSAH

Figure 2 shows the variation of molecular weight with the alkynyl-CTA concentration, which confirms that the molar masses of PMEDSAH directly correlate with the chain transfer agent concentration[19]. The molecular weight rises with the fall of CTA concentration. It is recognized that adding CTA to the polymerization system will result in the decrease of the reaction rate and molecular weight but the improvement of the controllability. It is found that the RAFT-mediated process prevail over the normal radical polymerization as the CTA concentration increased[20, 21].

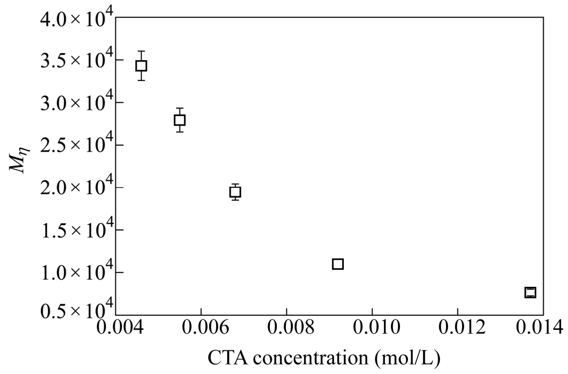

Fig. 2 Relationship between alkynyl terminated CTA concentration and the viscosity average molecular weight (M_η)

Coupling Alkynyl-PMEDSAH to MPPM-N$_3$ by Click Reaction

The route to combining click reaction with RAFT polymerization to graft MEDSAH onto the membrane surface is presented in Fig. 3. Br atoms were tethered to the membrane (MPPM-Br) *via* bromination under UV radiation[22, 23]; then they were substituted with triazos to obtain a clickable membrane (MPPM-N$_3$)[10]; finally, alkynyl-PMEDSAH was coupled to MPPM-N$_3$ *via* the Cu^I-catalyzed click reaction between alkynyl and triazo. The combination of click chemistry and RAFT polymerization technique was adopted from our previous work to modify MPPM and polyamide forward osmosis membranes; however,

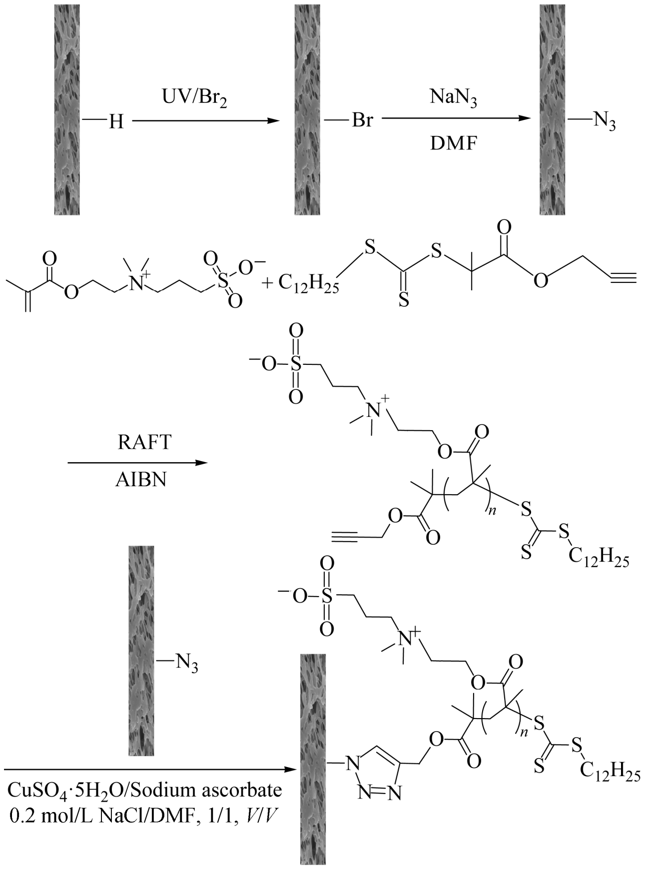

Fig. 3 Surface modification of MPPM by using RAFT technique and click chemistry

the effects of the grafting density and grafting chain length on the membrane characteristics were not investigated. Herein, the impacts of the grafting branch chain length (degree of polymerization) and the grafting density (grafting chains per membrane area) on the permeation performances of the modified membranes are two highlights in our present work.

Alkynyl-PMEDSAH is insoluble in deionized-water while soluble in 0.2 mol/L NaCl solution, and alkynyl-PMEDSAH aqueous solution is viscous. Moreover, MPPM is hydrophobic and cannot be wetted in pure water. Therefore, we utilized a mixture medium of 0.2 mol/L NaCl aqueous solution and DMF (1/1, *V*/*V*) for the click reaction.

The effect of polymer concentration on grafting density is shown in Fig. 4. The grafting density increases with the increase of alkynyl-PMEDSAH concentration. With an increase in the concentration, more and more alkynyl-PMEDSAH chains have access to the reactive sites, leading to the increase of grafting density.

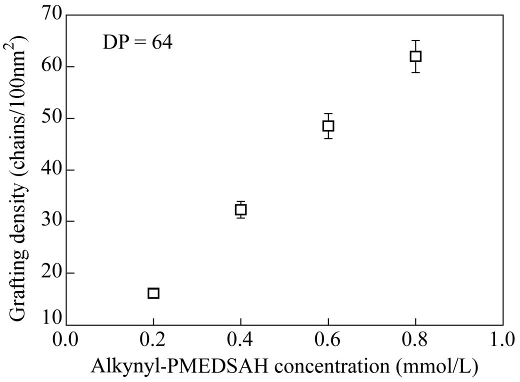

Fig. 4 Variation of grafting density with alkynyl-PMEDSAH concentration

Surface Characterization

Figure 5 displays the XPS spectra of the virgin and modified MPPM surfaces. The O1s peaks (Figs. 5a and 5b) show that the virgin MPPM and MPPM-Br contain some O_2 element on their surfaces, which may result from the oxidation under natural condition[24] and UV oxidation[22], respectively. Br3d5, Br3p3 and Br3s peaks appear at 72.0, 185.0 and 259.0 eV respectively in the wide scan XPS of MPPM-Br[22]. Br signal intensity weakens and an N1s signal appears at 402.3 eV (Fig. 5c), which confirms that triazo successfully substitutes Br atoms. After coupling alkynyl-PMEDSAH to MPPM-N_3 surface (Figs. 5d–5f), a new peak assigned to S2p3 appears at 166.0 eV; the N1s strengthens in comparison with MPPM-N_3, indicating grafting PMEDSAH to the membrane surface successfully.

To further distinguish the different functional groups from XPS spectra, the C1s, O1s, N1s envelopes were analyzed and peak-fitted (Fig. 5). The detailed attribution can be referred to the literature[25]. C1s spectrum for the virgin has peaks assigned to $\underline{C}-C$ or $\underline{C}-H$ (284.7 eV), $\underline{C}-O$ (285.8 eV) and $\underline{C}=O$ (287.5 eV). The peaks located at 537.5 eV for $\underline{O}-C$, 539.2 eV for $\underline{O}=C$, appear. The N1s spectrum has two distinct peaks centered at 401.6 and 404.0 eV, attributable to $\underline{N}-C/\underline{N}-H$ and $\underline{N}=$, $-N-\underline{N}=N$ atoms in

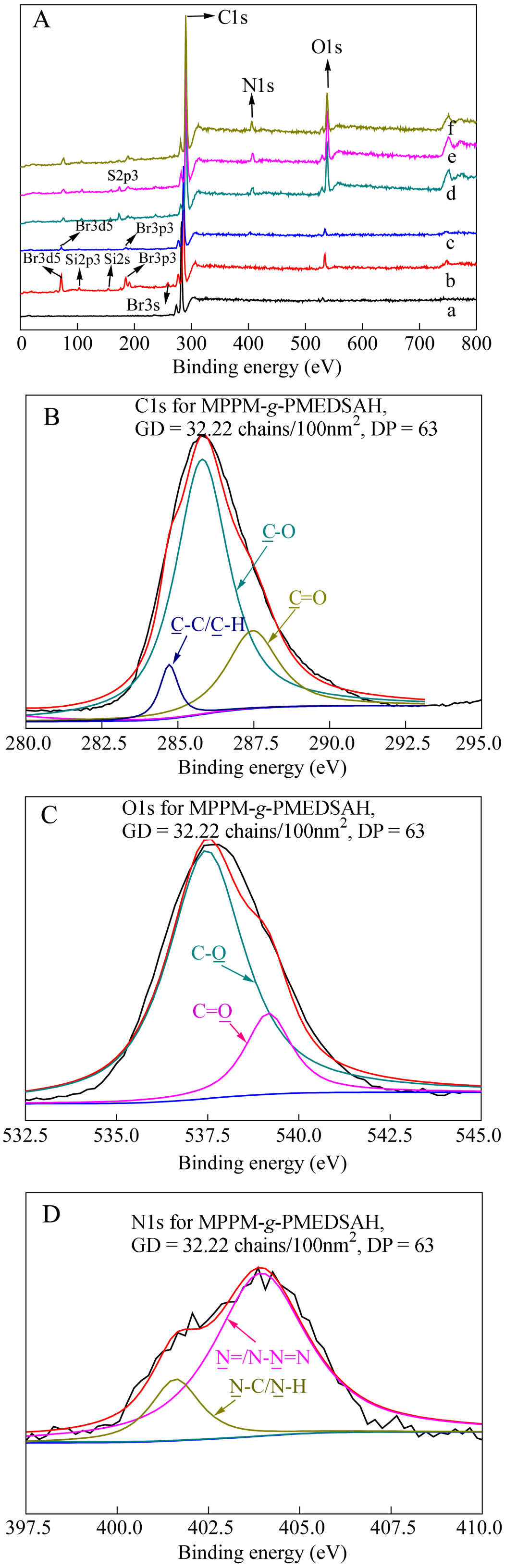

Fig. 5 (A) Wide scan XPS spectra for the unmodified and modified MPPMs: (a) the nascent, (b) MPPM-Br, (c) MPPM-N_3, (d) MPPM-*g*-PMEDSAH, GD = 32.22 chains/100nm^2, DP = 63, (e) MPPM-*g*-PMEDSAH, GD = 48.52 chains/100nm^2, DP = 91, (f) MPPM-*g*-PMEDSAH, GD = 61.98 chains/100nm^2, DP = 112; Others: the high-resolution spectra for (B) C1s, (C) O1s and (D) N1s

https://doi.org/10.1007/s10118-018-2013-2

the triazole ring, respectively[26]. These analyses also confirm the successful clicking PMEDSAH onto the membrane surface.

The element molar content of the samples is summarized in Table 1. Br molar content descends and N ascends obviously after the S_N2 substitution. The O/C ratio is 1.09% for the virgin membrane, indicating that the virgin membrane is slightly oxidized[27]. The atomic ratios of O/C and Br/C increase respectively from 1.09 mol% to 5.35 mol% and from 0 mol% to 3.62 mol%, suggesting that UV bromination brought about O and Br elements. N/C molar ratio increases from 0 mol% to 0.90 mol% while Br/C descends from 3.62 mol% to 1.82 mol%, which demonstrate that bromine is successfully exchanged with triazo. The atomic ratio of S/C decreases, indicating that more PMEDSAH was grafted to the membrane effectively.

Figure 6 presents the surface morphologies of MPPMs. It can be found that the unmodified MPPM has a porous and clear surface; the modified MPPMs are more or less covered with polymers; the membrane pores shrink, and surface porosity reduces along with the grafting density.

Water Contact Angle Measurements

Membrane surface hydrophilicity can be easily determined *via* water contact angle measurement[28]. The water contact angles on the membrane surfaces at all modification stages are presented in Fig. 7. The highest water contact angle is 105.2° on the unmodified membrane surface. It reduces to about 78.5° on the modified membrane surface with a low grafting density of PMEDSAH (GD of 32.22 chains/100nm^2); it further falls to 51.5° for the PMEDSAH grafted membrane with a grafting density of 61.98 chains/100nm^2, since a hydration layer could be formed due to electrostatic interaction and hydrogen bond[29].

Permeation Properties of the Membranes

It is well recognized that hydrophilic modification with a hydration layer could make the hydrophobic membrane much more repellent to fouling. As shown in Table 2, the pure water flux increases along with the branch chain length (degree of polymerization) and grafting density (grafting chains per membrane area), because the surface hydrophilicity was improved after grafting more PMEDSAH chains to the membrane.

The membrane performance was studied as functions of the grafting density and the degree of polymerization by the ultrafiltration of BSA solution (Table 2). It is observed that the flux decreases dramatically due to the fact that protein molecules can adsorb onto membrane surfaces as well as into the pores[30]. A relatively steady flux after about 15 min is obtained, which results from the saturation of the protein adsorption. As seen from Figs. 8 and 9, the normalized water flux of BSA solution increases along with the grafting density and the branch chain length up to the GD of

Table 1 Elemental content of different MPPM samples

Membrane	Element content (%)					Atomic ratio (%)			
	O	Br	N	S	C	O/C	Br/C	N/C	S/C
Blank MPPM				–	–	1.09	–	–	–
MPPM-Br (36.39 Br atoms/100nm^2) [a]	91.77	4.91	3.32	–	–	5.35	3.62	–	–
MPPM-N_3 (24.96 triazos/100nm^2) [b]	94.27	3.16	1.72	0.85	–	3.35	1.82	0.90	–
MPPM-*g*-PMEDSAH, DP = 63	78.53	14.84	1.17	3.71	1.75	18.90	1.49	4.72	2.23
MPPM-*g*-PMEDSAH, DP = 91	80.72	12.70	1.03	4.10	1.46	15.73	1.28	5.08	1.81
MPPM-*g*-PMEDSAH, DP = 112	84.27	9.81	1.41	3.79	0.71	11.64	1.67	4.50	0.84

[a] Grafting density of bromines on the membrane is calculated by the following formula: GD (bromines/100nm^2) = $(m_1 - m_0)/(A_{BET} \times 79.904) \times (10^{23}/10^{18}) \times 100$;
[b] Grafting density of triazos on the membrane is calculated by the following formula: GD (triazos/100nm^2) = $-(m_2 - m_1)/(A_{BET} \times 42) \times (10^{23}/10^{18}) \times 100$, where m_0 is the weight of the nascent membrane, m_1 the weight of MPPM-Br, 79.904 atomic weight of Br, m_2 the weight of the MPPM-N_3, 42 the total atomic weight of triazos, "–" means reduction of the weights before and after triazo functionalization. All the results were the average of three parallel experiments.

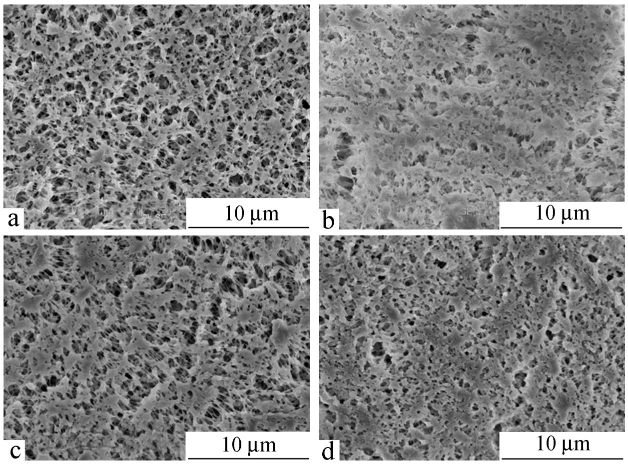

Fig. 6 FESEM images for (a) the nascent, (b) MPPM-Br, (c) MPPM-N_3 and (d) MPPM-*g*-PMEDSAH (GD = 61.98 chains/100nm^2, DP is 80.)

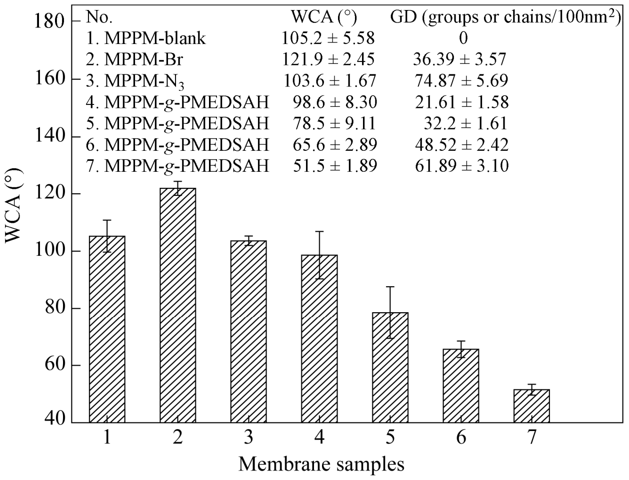

Fig. 7 Water contact angle on different membrane surfaces (DP is 80 for all the PMEDSAH modified membranes.)

Table 2 Effects of the grafting density (GD) and degree of polymerization (DP, repeating units) or branch chain length on the pure water flux (LMH), relative flux reduction (RFR), flux recovery ratio (FRR), reversible and irreversible fouling

Membrane		Flux	Flux changes		Fouling	
GD (chain/100nm^2)	DP	Pure water flux (L/(m^2·h))	FRR (%)	RFR (%)	Reversible fouling (%)	Irreversible fouling (%)
0	0	400.0	43.0	63.5	6.5	57.0
16.11	64	268.0	42.2	60.2	2.4	57.8
21.61	64	468.0	45.3	57.2	2.5	54.7
32.22	64	544.0	49.1	63.6	12.7	50.9
48.52	64	780.0	71.3	69.7	41.0	28.7
61.98	64	948.0	77.5	38.4	15.9	22.5
20.47	24	500.0	43.2	56.9	0.1	56.8
28.62	35	656.0	44.3	55.8	0.1	55.7
61.98	63	904.0	48.9	63.4	12.3	51.1
84.35	91	1056.0	68	62.7	30.7	32.0
100.84	112	1132.0	73.3	55.1	28.4	26.7

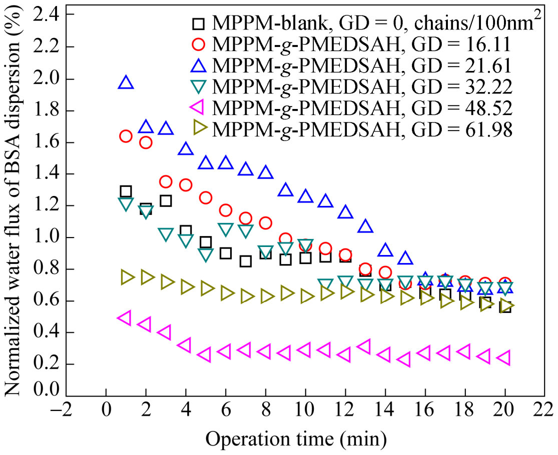

Fig. 8 Effect of the grafting density on the normalized water flux of BSA dispersion (DP is 64 for all the PMEDSAH modified membranes.)

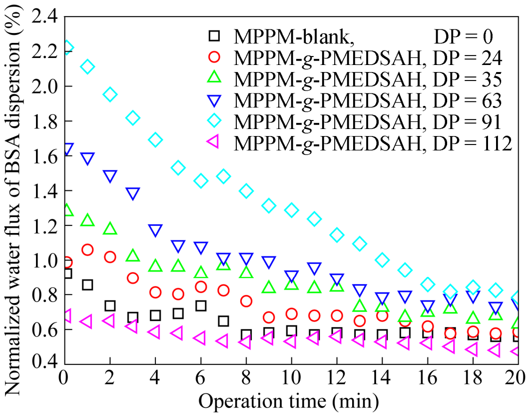

Fig. 9 Effect of the degree of polymerization on the normalized water flux of BSA dispersion (PMEDSAH concentration = 0.8 mmol/L.)

21.61 chains/100nm^2 and DP of 91. The increase is owing to the improvement of the membrane surface hydrophilicity and the chain movement in the solution to prevent the foulants from approaching the membrane surface. The decrease of the water flux of BSA solution when GD and DP are higher than 21.61 chains/100nm^2 and DP of 91 is due to the pore blocking. BSA rejection ascends with the grafting density consequently (Fig. 10) due to the membrane pore size shrinking with the increase of grafting density.

The relative flux reduction (RFR) declines while flux recovery ratio (FRR) enhances concurrently with grafting density (Table 2). The water flux just retrieves to 43.0% for the virgin MPPM but to 77.5% for the PMEDSAH grafted MPPM. The irreversible fouling ratios are 57.0% and 22.5% for the unmodified membrane and the modified membrane (GD 61.98 chains/100nm^2, DP 64), respectively. The reversible fouling ratios are 6.5% and 41.0% for the unmodified membrane and the modified membrane (GD 48.52 chains/100nm^2, DP 64), respectively. In general, the irreversible fouling is much serious to the unmodified MPPM, but it could be greatly restrained by the grafting of PMEDSAH chains onto the membrane surface.

Grafting density (grafting chains per membrane area, GD) and grafting branch chain length (degree of polymerization, DP) play important parts in determining the membrane performance. To find out the relations of GD and DP with the pure water flux, FRR, RFR, reversible and irreversible fouling, Pearson correlations (r_{xy}) were calculated by SPSS 19.0 (Table 3).

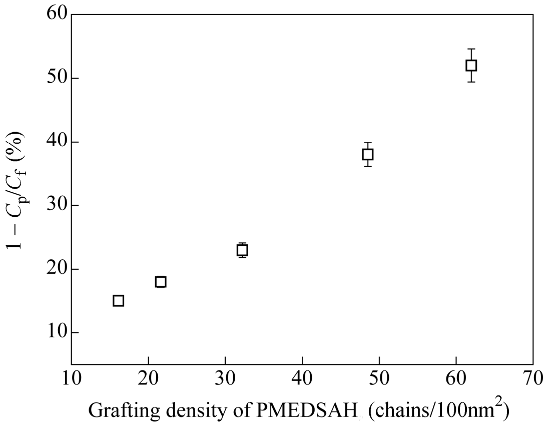

Fig. 10 Effect of the grafting density of PMEDSAH on the rejection of BSA dispersion
The rejection of BSA dispersion is defined as 1 − C_p/C_f, where C_p and C_f is the BSA concentration in the permeate and the feed dispersion. DP = 64.23 or M_η = 1.95 × 10^4.

https://doi.org/10.1007/s10118-018-2013-2

Table 3 Pearson correlation between the grafting density (GD), degree of polymerization (DP) and the pure water flux, relative flux reduction (RFR), flux recovery ratio (FRR), reversible and irreversible fouling

	Pure water flux	FRR	RFR	Reversible fouling	Irreversible fouling
GD	0.956^{**}	0.806^{**}	–0.185	0.714^{*}	$–0.806^{**}$
DP	0.670^{*}	0.648^{*}	–0.088	0.609^{*}	$–0.648^{*}$

*Correlation is significant at the 0.05 level (2-tailed); **Correlation is significant at the 0.01 level (2-tailed).

$$r_{xy}=\frac{\sum_{i=1}^{i=n}\left(x_i-\bar{x}\right)\left(y_i-\bar{y}\right)}{\sqrt{\sum_{i=1}^{i=n}\left(x_i-\bar{x}\right)^2\left(y_i-\bar{y}\right)^2}} \tag{7}$$

where y is experimental value of GD and DP, y_i number i of y; x the pure water flux, FRR and RFR, reversible and irreversible fouling, x_i number i of x.

Results demonstrate that Pearson correlations between GD, DP and the pure water flux (0.956^{**} and 0.670^{*}), FRR (0.806^{**} and 0.648^{*}), reversible fouling (0.714^{*} and 0.609^{*}) are positively significant. Meanwhile, Pearson correlations between GD, DP and irreversible fouling ($–0.806^{**}$ and $–0.648^{*}$) are negatively significant. The results indicate that the larger the coverage of PMEDSAH on the membrane surface and the longer the grafting branch chain length are, the higher the water flux and the better the antifouling characteristics of the membranes will be. From Table 3, a conclusion can be drawn that GD plays a more important role than DP does. In our previous work, we found that grafting density and pendent length play equally important roles in membrane fouling[31]. This may be caused by the experimental errors.

Pearson correlations between GD, DP and RFR are negative but not significant (–0.185 and –0.088), indicating that the higher the coverage of PMEDSAH on the membrane surface and the longer the grafting branch chain length are, the lower the RFR is, and hence the better the antifouling characteristics will be. The results demonstrate that GD and DP play trivial roles in RFR. Whether or not the membrane is modified the cake formation on the surface results in the reduction of the pure water flux[32]. The negative correlation also confirms our previous results that the hydrophilicity of the surface reduces hydraulic resistance, improves the flow rate, and leads to formation of a secondary membrane due to cake formation and compaction. The secondary membrane brings about the increase of resistance and decrease of flow rate[33, 34]. It can also be seen from Figs. 8 and 9 that the gap between the pure water fluxes becomes narrower in the filtration process, and the fluxes are very close to each other during the steady stage. This result indicates that the secondary membrane dominates the filtration process while the membrane itself functions only as a supporting layer.

CONCLUSIONS

MPPM-*g*-PMEDSAH membranes with well-controlled grafting branch chain lengths and grafting densities were prepared by combining RAFT polymerization technique with click reaction. XPS analyses confirmed that PMEDSAH was successfully introduced to MPPM. The water contact angle decreased with the grafting density increasing. The filtration experimental results demonstrated that the extent of protein fouling could be alleviated significantly by PMEDSAH grafting. Pearson correlation analysis showed that the pure water flux and the flux recover ratio were positively correlated with the branch chain length and grafting density, that is, the modified membranes with high grafting density and long branch chain length possess the better antifouling characteristics.

ACKNOWLEDGMENTS

This work was financially supported by the National Natural Science Foundation of China (No. 21371008).

REFERENCES

1 Dai, Q. W.; Xu, Z. K.; Deng, H. T.; Liu, Z. M.; Wu, J.; Seta, P. Surface modification of microporous polypropylene membranes by graft polymerization of *N*,*N*-dimethylaminoethyl methacrylate. Chinese J. Polym. Sci. 2004, 22(4), 369–377.

2 Jaleh, B.; Parvin, P.; Wanichapichart, P.; Saffar, A. P.; Reyhani, A. Induced super hydrophilicity due to surface modification of polypropylene membrane treated by O_2 plasma. Appl. Surf. Sci. 2010, 257(5), 1655–1659.

3 Yang, Q.; Xu, Z. K.; Dai, Z. W.; Wang, J. L.; Ulbricht, M. Surface modification of polypropylene microporous membranes with a novel glycopolymer. Chem. Mater. 2005, 17(11), 3050–3058.

4 Liu, Z. M.; Xu, Z. K.; Ulbricht, M. Surface modification of polypropylene microporous membrane by tethering polypeptides. Chinese J. Polym. Sci. 2006, 24(5), 529–538.

5 Ma, G. Q.; Zhai, J. J.; Liu, B.; Huang, D. H.; Sheng, J. Plasma modification of polypropylene surfaces and grafting copolymerization of styrene onto polypropylene. Chinese J. Polym. Sci. 2012, 30(3), 423–435.

6 Yang, Q.; Tian, J.; Xu, Z. K. Photo-induced graft polymerization of acrylamide on polypropylene membrane surface in the presence of dibenzyl trithiocarbonate. Chinese J. Polym. Sci. 2007, 25(2), 221–226.

7 Meng, J. Q.; Yuan, T.; Kurth, C. J.; Shi, Q.; Zhang, Y. F. Synthesis of antifouling nanoporous membranes having tunable nanopores *via* click chemistry. J. Membr. Sci. 2012, 401-402, 109–117.

8 Semsarilar, M.; Ladmiral, V.; Perrier S. Highly branched and hyperbranched glycopolymers *via* reversible addition-fragmentation chain transfer polymerization and click chemistry. Macromolecules 2010, 43(3), 1438–1443.

9 Khabibullin, A.; Bhangaonkar, K.; Mahoney, C.; Lu, Z.; Schmitt, M.; Sekizkardes, A. K.; Bockstaller, M. R.; Matyjaszewski, K. Grafting PMMA brushes from alpha-alumina nanoparticles *via* SI-ATRP. ACS Appl. Mater. Interfaces 2016, 8(8), 5458–5465.

10 Wu, X. M.; Wang, L. L.; Wang, Y.; Gu, J. S.; Yu, H. Y. Surface modification of polypropylene macroporous membrane by marrying RAFT polymerization with click chemistry. J. Membr. Sci. 2012, 421-422, 60–68.

11 Lalani, R.; Liu, L. Synthesis, characterization, and electrospinning of zwitterionic poly(sulfobetaine methacrylate). Polymer 2011, 52(23), 5344–5354.

12 Ladd, J.; Zhang, Z.; Chen, S.; Hower, J. C.; Jiang, S. Zwitterionic polymers exhibiting high resistance to nonspecific protein adsorption from human serum and plasma. Biomacromolecules 2008, 9(5), 1357–1361.

13 Vogler, E. A. Structure and reactivity of water at biomaterial surfaces. Adv. Colloid Interf. Sci. 1998, 74, 69–117.

14 Zhang, Z.; Zhang, M.; Chen, S.; Horbett, T. A.; Ratner, B. D.; Jiang, S. Blood compatibility of surfaces with superlow protein adsorption. Biomaterials 2008, 29(32), 4285–4291.

15 Shih, Y. J.; Chang, Y. Tunable blood compatibility of polysulfobetaine from controllable molecular-weight dependence of zwitterionic nonfouling nature in aqueous solution. Langmuir 2010, 26(22), 17286–17294.

16 Yu, H.Y.; Kang, Y.; Liu, Y. L.; Mi, B. X. Grafting polyzwitterions onto polyamide by click chemistry and nucleophilic substitution on nitrogen: a novel approach to enhance membrane fouling resistance. J. Membr. Sci. 2014, 449, 50–57.

17 Ranjan, R.; Brittain, W. J. Combination of living radical polymerization and click chemistry for surface modification. Macromolecules 2007, 40(40), 6217–6223.

18 Yadav, S. K.; Yoo, H. J.; Cho, J. W. Click coupled graphene for fabrication of high-performance polymer nanocomposites. J. Polym. Sci., Part B: Polym. Phys. 2013, 51(1), 39–47.

19 Barbey, R.; Perrier, S. Synthesis of polystyrene-based hyperbranched polymers by Thiol-Yne chemistry: a detailed investigation. Macromolecules 2014, 47(19), 6697–6705.

20 Ying, L.; Yu, W. H.; Kang, E. T.; Neoh, K. G. Functional and surface-active membranes from poly(vinylidene fluoride)-graft-poly(acrylic acid) prepared *via* RAFT-mediated graft copolymerization. Langmuir 2004, 20(14), 6032–6040.

21 Yu, H. Y.; Li, W.; Zhou, J.; Gu, J. S.; Huang, L.; Tang, Z. Q.; Wei, X. W. Thermo- and pH-responsive polypropylene microporous membrane prepared by the photoinduced RAFT-mediated graft copolymerization. J. Membr. Sci. 2009, 343(1-2), 82–89.

22 Balamurugan, S.; Mandale, A.; Badrinarayanan, S.; Vernekar, S. Photochemical bromination of polyolefin surfaces. Polymer 2001, 42(6), 2501–2512.

23 Chanunpanich, N.; Ulman, A.; Strzhemechny, Y.; Schwarz, S.; Janke, A.; Braun, H.; Kraztmuller, T. Surface modification of polyethylene through bromination. Langmuir 1999, 15(6), 2089–2094.

24 Song, L.; Zhao, J.; Yang, H.; Jin, J.; Li, X.; Stagnaro, P.; Yin, J. H. Biocompatibility of polypropylene non-woven fabric membrane *via* UV-induced graft polymerization of 2-acrylamido-2-methylpropane sulfonic acid. Appl. Surf. Sci. 2011, 258(1), 425–430.

25 Wu, X. M.; Wang, L. L.; Wang, Y.; Gu, J. S.; Yu, H. Y. Surface modification of polypropylene macroporous membrane by marrying RAFT polymerization with click chemistry. J. Membr. Sci. 2012, 421, 60–68.

26 Cai, T.; Neoh, K.G.; Kang, E.T. Poly(vinylidene fluoride) graft copolymer membranes with “clickable” surfaces and their functionalization. Macromolecules 2011, 44(11), 4258–4268.

27 Rjeb, A.; Letarte, S.; Tajounte, L.; El Idrissi, M. C.; Adnot, A.; Roy, D.; Claire, Y.; Kaloustian, J. Polypropylene natural aging studied by X-ray photoelectron spectroscopy. J. Electron Spectrosco. 2000, 107(3), 221–230.

28 Yue, W. W.; Li, H. J.; Xiang, T.; Qin, H.; Sun, S. D.; Zhao, C. S. Grafting of zwitterion from polysulfone membrane *via* surface-initiated ATRP with enhanced antifouling property and biocompatibility. J. Membr. Sci. 2013, 446, 79–91.

29 Zhang, Z.; Chen, S.; Chang, Y.; Jiang, S. Surface grafted sulfobetaine polymers *via* atom transfer radical polymerization as superlow fouling coatings. J. Phys. Chem. 2006, 110(22), 10799–10804.

30 Li, L.; Yin, Z.; Li, F.; Xiang, T.; Chen, Y.; Zhao, C. Preparation and characterization of poly(acrylonitrile-acrylic acid-*N*-vinyl pyrrolidinone) terpolymer blended polyethersulfone membranes. J. Membr. Sci. 2010, 349(1), 56–64.

31 Wang, L. L.; Wu, J. J.; Zhang, Z. B.; Zhou, J.; He, X. C.; Yu, H. Y.; Gu, J. S. Methoxypolyethylene glycol grafting on polypropylene membrane for enhanced antifouling characteristics: effect of pendant length and grafting density. Sep. Purif. Technol. 2016, 164, 81–88.

32 Belfer, S.; Fainshtain, R.; Purinson, Y.; Gilron, J.; Nystrom, M.; Manttari, M. Modification of NF membrane properties by *in situ* redox initiated graft polymerization with hydrophilic monomers. J. Membr. Sci. 2004, 239(1), 55–64.

33 le Roux, I.; Krieg, H. M.; Yeates, C. A.; Breytenbach, J. C. Use of chitosan as an antifouling agent in a membrane bioreactor. J. Membr. Sci. 2005, 248(1-2), 127–136.

34 Yu, H. Y.; He, X. C.; Liu, L. Q.; Gu, J. S.; Wei, X. W. Surface modification of polypropylene microporous membrane to improve its antifouling characteristics in an SMBR: N_2 plasma treatment. Water Res. 2007, 41(20), 4703–4709.

https://doi.org/10.1007/s10118-018-2013-2